# The effect of pressure and substituents on the size of pseudo-macrocyclic cavities in salicylaldoxime ligands

**Post-print of a peer-reviewed article published by the Royal Society of Chemistry.**
**Published article available at: http://dx.doi.org/10.1039/B712397C**

**Cite as:**
**Wood, P. A., Forgan, R. S., Lennie, A. R., Parsons, S., Pidcock, E., Tasker, P. A., & Warren, J. E. (2008). The effect of pressure and substituents on the size of pseudo-macrocyclic cavities in salicylaldoxime ligands. *CrystEngComm*, 10(2), 239-251.**

**Manuscript received: 13/08/2007; Accepted: 15/10/2007; Article published: 31/10/2007**

# The Effect of Pressure and Substituents on the Size of Pseudo-Macrocyclic Cavities in Salicylaldoxime Ligands**

Peter A. Wood,[1] Ross S. Forgan,[1] Alistair R. Lennie,[2] Simon Parsons, [1,]* Elna Pidcock,[2]
Peter A. Tasker, [1,]* John E. Warren[3]

[1]EaStCHEM, School of Chemistry, Joseph Black Building, University of Edinburgh, West Mains Road, Edinburgh, EH9 3JJ, UK.

[2]Cambridge Crystallographic Data Centre, 12 Union Road, Cambridge, CB2 1EZ, UK.

[3]CCLRC, Daresbury Laboratory, Warrington, Cheshire, WA4 4AD, UK.

[*]Corresponding author; e-mail: s.parsons@ed.ac.uk, tel: +44-(0)131 650 4806,
fax: +44-(0)131 650 4743

[**]We are very grateful to Prof. Angelo Gavezzotti (University of Milan) for his help and advice with our PIXEL calculations. We also thank the EPSRC and The Cambridge Crystallographic Data Centre for funding, and the CCLRC for provision of synchrotron beam-time.

**Supporting information:**
CCDC reference numbers 656839–657083. For crystallographic data in CIF or other electronic format see http://dx.doi.org/10.1039/B712397C

***Abstract***

The effect of pressure on the crystal structures of 3-chloro-, 3-methoxy, 3-methyl and 3-*tert*-butylsalicylaldoximes has been investigated. The compounds all form the dimeric structure found in salicylaldoxime form I at ambient pressure, which is based on *inter*molecular hydrogen bonds between the oximic hydrogen and the phenolic oxygen atoms across an inversion centre. These *inter*molecular interactions, along with *intra*molecular phenolic hydrogen to oximic nitrogen atom hydrogen bonds form a pseudo-macrocycle with a $R_4^4(10)$ ring motif. These hydrogen bonding motifs pre-organize an arrangement of four potential donor atoms for a metal cation which, when the phenol groups are deprotonated, provides an $N_2O_2^{2-}$ pocket well suited to the binding of planar transition metal ions. The radius of the cavity defined by the donor atoms in the dimers is dependent on the nature of the 3-substituent, varying from 1.949 Å in the 3-methoxy- to 2.037 Å in the 3-$^t$Bu-derivative. Anisotropic compression of the crystals on the application of pressure results in significant changes in the radii of the cavities in the dimers which decrease by *ca.* 10% at 6 GPa. During compression of the 3-$^t$Bu-derivative a single crystal to single crystal phase transition was observed between 0.2 and 1.0 GPa to a new polymorph, 3-*tert*-butylsalicylaldoxime-II. The phase transition produces an increase in symmetry as the space group changes from *P*-1 to *I*2/*a*, but the intermolecular interactions remain essentially unchanged. No phase transitions were observed in the compression of 3-Cl-, 3-Me- or 3-MeO-salicylaldoxime up to 6.2 GPa.

***Introduction***

The use of hydrostatic pressure as a technique for modifying the local geometry of small molecular crystal structures is a rapidly expanding field. Much recent work has shown that pressure can be used to induce polymorphism,[1] adjust intermolecular interactions[2] and tune the size of intermolecular voids.[3] The voids found within the crystal structure at ambient conditions have been found to have a significant influence on the effects of pressure, with the primary consequences of compression tending to be reduction of these voids.

The voids, or cavities, in a structure can also be of considerable importance in terms of the properties and reactivity of the compound. Examples of this include nanoporous dipeptide structures that can host organic solvents,[4] clathrate compounds which can encapsulate larger molecules[5] and crown ethers, such as 18-crown-6 which forms different types of complex with $Na^+$, $K^+$ and $Rb^+$ due to the relative sizes of the ions compared to the intramolecular cavity within the crown ether.[6]

Salicylaldoxime [Scheme 1a] forms hydrogen bonded dimers, both in solution and in the solid state, which create a pseudo-macrocyclic cavity within the hydrogen bonded ring motif [Scheme 2]. The compound can form bis-salicylaldoximato complexes with transition metal ions by deprotonation of the phenol groups. The bis complex is further stabilised by hydrogen bonding between the two bidentate ligands. Salicylaldoxime is

known to be highly selective for complex formation of copper(II) over other transition metal ions due to the compatibility of the ionic radius of $Cu^{2+}$ with the size of the intermolecular cavity within the hydrogen bonded ring.[7] As a result of this, derivatives of salicylaldoxime are used as solvent extractants in the hydrometallurgical recovery of copper, a process which accounts for around a third of annual production.[8]

In a recent study of phase I of salicylaldoxime we showed that the size of the pseudo-macrocyclic cavity formed in the centre of the hydrogen bonded dimer can be reduced by the application of pressure.[9] The ligands used industrially for copper solvent extraction are salicylaldoximes derivatives incorporating substituents at different points of the molecule, principally to impart kerosene solubility, but it is known that such substituents also influence extractant strength and selectivity.[10] In this paper we consider how the effects of the application of pressure and of changing the nature of substituents close to the metal binding site influence the structure in the solid state and the size of the pseudo-macrocyclic cavity available to a metal ion. The compounds studied were 3-chlorosalicylaldoxime, 3-methylsalicylaldoxime, 3-methoxysalicylaldoxime and 3-*tert*-butylsalicylaldoxime and results are compared with those for unsubstituted salicylaldoxime.[9]

## *Experimental*

### *General comments*

All solvents and reagents were used as received from Aldrich and Fisher. $^{1}H$ and $^{13}C$ NMR were obtained using a Bruker AC250 spectrometer at ambient temperature. Chemical shifts (δ) are reported in parts per million (ppm) relative to internal standards. Hydrogen numbering in $^{1}H$ NMR data refers to Scheme I (a-e). Fast atom bombardment mass spectrometry (FABMS) was carried out using a Kratos MS50TC spectrometer with a thioglycerol matrix. Analytical data were obtained using a Carlo Erba CHNS analyser at the EastChem Microanalytical Service.

### *Synthesis*

3-methylsalicylaldoxime, 3-methoxysalicylaldoxime, 3-chlorosalicylaldoxime and 3-*tert*-butylsalicylaldoxime (Scheme I) were synthesised according to the literature method.[11]

**Oximation General Procedure.** Equivalents of KOH and $NH_2OH.HCl$ were dissolved separately in EtOH, mixed thoroughly and a white KCl precipitate removed by filtration. The filtrate was added to the precursor aldehyde, refluxed for 3 hr and the solvent removed in vacuo. The residue was redissolved in $CHCl_3$, washed with water 3 times, dried over $MgSO_4$ and the solvent removed *in vacuo* to yield the crude product.

**3-Chlorosalicylaldoxime.** Using the general procedure, 3-chlorosalicylaldehyde[12] (0.431 g, 2.75 mmol) was reacted with KOH (0.169 g, 3.0 mmol) and $NH_2OH.HCl$ (0.209 g, 3.0 mmol) to yield a white powder (0.376 g, 80 %). (Anal. Calc. for $C_7H_6ClNO_2$: C, 49.0; H, 3.5; N, 8.2. Found: C, 49.4; H, 3.1; N, 8.0 %); $^1$H NMR (250 MHz, $CDCl_3$): $\delta_H$ (ppm) 6.78 (t, 1H, Ar-H8), 7.05 (dd, 1H, Ar-H9), 7.30 (dd, 1H, Ar-H7), 8.15 (s, 1H, ArCHN); $^{13}$C NMR (63 MHz, $CDCl_3$) $\delta_C$ (ppm) 117.0 (1C, aromatic **C**-CHN), 121.0 (1C, aromatic **C**H), 122.0 (1C, aromatic **C**-Cl), 129.5 (1C, aromatic **CH**), 132.0 (1C, aromatic **C**H), 153.0 (1C, Ar**C**HN), 154.0 (1C, aromatic **C**-OH; FABMS m/z 172 $(MH)^+$, 100 %.

**3-Methylsalicylaldoxime.** Using the general procedure, 3-methylsalicylaldehyde (Aldrich, 1.000 g, 7.35 mmol) was reacted with KOH (0.425 g, 7.6 mmol) and $NH_2OH.HCl$ (0.530 g, 7.6 mmol) to yield a white powder, which was recrystallised from hexane to give colourless needles (0.889 g, 80 %). (Anal. Calc. for $C_8H_9NO_2$: C, 63.6; H, 6.0; N, 9.3. Found: C, 63.2; H, 6.0; N, 9.4%); $^1$H NMR (250 MHz, $CDCl_3$): $\delta_H$ (ppm) 2.20 (s, 3H, $ArCH_3$), 6.75 (t, 1H, Ar-H8), 6.95 (dd, 1H, Ar-H7), 7.08 (dd, 1H, Ar-H9); $^{13}$C NMR (63 MHz, $CDCl_3$) $\delta_C$ (ppm) 14.5 (1C, Ar**C**$H_3$), 115.0 (1C, aromatic **C**-CHN), 118.5 (1C, aromatic **C**H), 125.0 (1C, aromatic **C**-CH3), 127.5 (1C, aromatic **C**H), 132.0 (1C, aromatic **C**H), 152.5 (1C, Ar**C**HN), 154.5 (1C, aromatic **C**-OH); FABMS m/z 152 $(MH)^+$, 83 %.

**3-Methoxysalicylaldoxime (O-vanillin oxime).** Using the general procedure, 3-methoxysalicylaldehyde (Aldrich, 3.00 g, 19.7 mmol) was reacted with KOH (1.35 g, 24.0 mmol) and $NH_2OH.HCl$ (1.42 g, 20.4 mmol) to yield an off-white powder, which was recrystallised from $H_2O$ to give white needles (2.61 g, 79 %). (Anal. Calc. for $C_8H_9NO_3$: C, 57.5; H, 5.4; N, 8.4. Found: C, 57.4; H, 5.6; N, 8.6 %); $^1$H NMR (250 MHz, $CDCl_3$): $\delta_H$ (ppm) 4.12 (s, 3H, $OCH_3$), 7.08 (m, 3H, 3 x ArH), 8.42 (s, 1H, ArCHN); $^{13}$C NMR (63 MHz, $CDCl_3$) $\delta_C$ (ppm) 56.5 (1C, O**C**H3), 113.0 (1C, aromatic **C**H), 117.0 (1C, aromatic C-**C**HN), 120.0 (1C, aromatic **C**H), 125.0 (1C, aromatic **C**H), 146.5 (1C, aromatic **C**-OH), 147.5 (1C, aromatic **C**-OCH3), 153.0 (1C, Ar**C**HN); FABMS m/z 168 $(MH)^+$, 91 %.

**3-*tert*-Butylsalicylaldoxime.** Using the general procedure, 3-tert-butylsalicylaldehyde (Aldrich, 2.50 g, 14.0 mmol) was reacted with KOH (1.35 g, 24.0 mmol) and $NH_2OH.HCl$ (1.42 g, 20.4 mmol) to yield a white powder, which was recrystallised from hexane to give white fluffy needles (2.34 g, 86 %). (Anal. Calc. for $C_{11}H_{15}NO_2$: C, 68.4; H, 7.8; N, 7.3. Found: C, 68.4; H, 8.3; N, 7.4 %); $^1$H NMR (250 MHz, $CDCl_3$): $\delta_H$ (ppm) 1.34 (s, 9H, $C(CH_3)_3$), 6.78 (t, 1H, Ar-H8*), 6.95 (dd, 1H, Ar-H7*), 7.22 (dd, 1H, Ar-H9*); $^{13}$C NMR (63 MHz, $CDCl_3$) $\delta_C$ (ppm) 29.5 (3C, C(**C**$H_3)_3$), 35.5 (1C, **C**$(CH_3)_3$), 117.0 (1C, aromatic **C**-CHN), 119.5 (1C,

aromatic **C**H), 129.5 (1C, aromatic **C**H), 130.0 (1C, aromatic **C**H), 138.0 (1C, aromatic **C**-C($CH_3$)$_3$), 154.5 (1C, Ar**C**HN), 157.0 (1C, aromatic **C**-OH); FABMS m/z 194 $(MH)^+$, 100 %.

*Crystal growth*

The samples were recrystallised by slow evaporation of a concentrated solution of hexane/chloroform (for 3-Me- and 3-$^t$Bu-salicylaldoxime), chloroform (for 3-Me-salicylaldoxime) or dichloromethane (for 3-Cl-salicylaldoxime). A colourless block of each compound was cut to the required dimensions for high pressure crystallography.

Initial pressure experiments on 3-chlorosalicylaldoxime showed that the crystals were made up of layers and upon application of pressure the crystals were inherently prone to shearing in the direction of these layers. This meant that it was very difficult to obtain high-quality compression data when using a single crystal cut from a larger sample. A crystal was therefore grown *in-situ* from solution by the application of hydrostatic pressure. A saturated solution in 4:1 methanol/ethanol was loaded into a diamond-anvil cell (see below). Pressure was increased to 0.2 GPa (at room temperature), leading to formation of several crystallites within the cell. The temperature was then increased until the polycrystalline sample began to redissolve. The temperature of the cell was then cycled around this elevated temperature in order to reduce the number of crystallites. Allowing the cell to cool to room temperature yielded a single crystal. Diffraction data were collected on the sample which could be indexed on essentially the same unit cell as the ambient pressure structure [monoclinic, $a$ = 13.076 (5), $b$ = 3.8514 (6), $c$ = 14.234 (3) Å, β = 91.75 (2) ° and $V$ = 716.5 (3) Å$^3$].

*High Pressure Crystallography*

Crystal structures at ambient temperature and pressure have been reported separately.[13]

High-pressure experiments were carried out using a Merrill-Bassett diamond anvil cell (half-opening angle 40°), equipped with brilliant-cut diamonds with 600μm culets and a tungsten gasket.[14] A 1:1 mixture of *n*-pentane and isopentane was used as a hydrostatic medium for 3-methyl-, 3-methoxy- and 3-*tert*-butylsalicylaldoxime; the 4:1 methanol/ethanol mother liquor from crystal growth (see above) was used for 3-chlorosalicylaldoxime. Due to the high volatility of the *n*-pentane/isopentane solution, the cells loaded with this medium were cooled in dry ice prior to loading. A small ruby chip was also loaded into each cell as the pressure calibrant, with the ruby fluorescence method being used to measure the pressure.[15] In the case of 3-chlorosalicylaldoxime, the crystal scattered relatively strongly and so data were collected on a Bruker-Nonius APEX-II diffractometer with graphite-monochromated, sealed-tube Mo-Kα radiation (λ = 0.71073 Å). For the remaining crystals diffraction data were collected on a Bruker-Nonius APEX-II diffractometer with silicon-

monochromated synchrotron radiation (λ = 0.4577 Å for the 3-Me- and λ = 0.4869 Å for the 3-MeO- and 3-*t*-Bu-compounds) on Station 9.8 at the SRS, Daresbury Laboratory.

Data collection and processing procedures for the high-pressure experiments followed previous studies.[16, 17] Integrations were carried out using the program SAINT,[18] and absorption corrections with the programs SHADE[19] and SADABS.[20] Data collections were taken in approximately 1.0 GPa steps from between 0.2 – 0.5 GPa up to the highest pressure at which usable data could be collected - between 5.0 and 6.2 GPa. Determination of the cell constants of 3-*tert*-butylsalicylaldoxime at 1.0 GPa showed that a single-crystal to single-crystal phase transition had occurred to a new polymorph, which we have designated 3-*tert*-butylsalicylaldoxime-II. The phase transition did not appear to cause significant degradation of the crystal quality, so the compression study was continued up to the limits of the hydrostatic medium. No phase transitions were found in the single crystal compression studies of the 3-chloro, 3-methyl or 3-methoxy-salicylaldoximes in the pressure ranges studied.

Refinements of the compressed forms of each compound were carried out starting from the co-ordinates determined at ambient pressure. The structure of the new phase of the *t*-butyl derivative (3-*tert*-butylsalicylaldoxime-II) was solved by direct methods using the program *SIR92* and refinements of the subsequent high-pressure datasets were carried out starting from these coordinates. Refinements were carried out against $|F|^2$ using all data (CRYSTALS).[21] Extreme outlier reflections (e.g. those partially cut-off by the pressure cell, or overlapping with diamond reflections or Be powder lines) were omitted from the refinement. Listings of crystal and refinement data are given in Table 1.

| | **Ambient** | **1.6 GPa** | **2.4 GPa** | **3.4 GPa** | **5.0 GPa** |
|---|---|---|---|---|---|
| Crystal data | | | | | |
| Chemical formula | $C_7H_6ClNO_2$ | $C_7H_6ClNO_2$ | $C_7H_6ClNO_2$ | $C_7H_6ClNO_2$ | $C_7H_6ClNO_2$ |
| $M_r$ | 171.58 | 171.58 | 171.58 | 171.58 | 171.58 |
| Cell setting, space group | Monoclinic, $P2_1/c$ | Monoclinic, $P2_1/c$ | Monoclinic, $P2_1/c$ | Monoclinic, $P2_1/c$ | Monoclinic, $P2_1/c$ |
| Temperature (K) | 298 | 298 | 298 | 298 | 298 |
| $a$, $b$, $c$ (Å) | 13.1506 (18), 3.8859 (6), 14.3115 (19) | 12.843 (3), 3.6613 (3), 13.7921 (16) | 12.748 (2), 3.5954 (3), 13.6496 (15) | 12.652 (4), 3.5295 (4), 13.509 (2) | 12.544 (6), 3.4424 (8), 13.365 (5) |
| β (°) | 91.548 (10) | 92.603 (13) | 93.115 (13) | 93.64 (2) | 94.44 (4) |
| $V$ (Å$^3$) | 731.08 (18) | 647.88 (16) | 624.71 (15) | 602.0 (2) | 575.4 (4) |
| $Z$ | 4 | 4 | 4 | 4 | 4 |
| $D_x$ (Mg m$^{-3}$) | 1.559 | 1.759 | 1.824 | 1.893 | 1.981 |
| | | | | | |
| Data collection | | | | | |
| No. of measured, independent and observed ($I$ > 2.00u($I$)) reflections | 10310, 1955, 1127 | 3158, 440, 348 | 3218, 415, 341 | 2720, 416, 319 | 3081, 351, 231 |
| $R_{int}$ | 0.018 | 0.064 | 0.060 | 0.076 | 0.098 |
| | | | | | |
| Refinement | | | | | |
| $R[F^2 > 2\sigma(F^2)]$, $wR(F^2)$, $S$ | 0.033, 0.083, 0.80 | 0.058, 0.158, 1.02 | 0.046, 0.121, 1.03 | 0.078, 0.227, 1.02 | 0.045, 0.123, 1.00 |
| No. of reflections | 1955 reflections | 440 reflections | 415 reflections | 409 reflections | 344 reflections |
| No. of parameters | 106 | 106 | 106 | 106 | 106 |
| $\Delta\rho_{max}$, $\Delta\rho_{min}$ (e Å$^{-3}$) | 0.21, –0.12 | 0.26, –0.22 | 0.25, –0.22 | 0.36, –0.40 | 0.33, –0.33 |
| Completeness to 0.83 Å | 99.9% | 35.7% | 35.4% | 36.9% | 32.3% |

***Table 1.*** (a) Crystallographic data for 3-chlorosalicylaldoxime at increasing pressures.

| | **Ambient** | **1.3 GPa** | **2.2 GPa** | **3.5 GPa** | **4.2 GPa** | **4.9 GPa** | **5.6 GPa** |
|---|---|---|---|---|---|---|---|
| Crystal data | | | | | | | |
| Chemical formula | $C_8H_9NO_2$ | $C_8H_9NO_2$ | $C_8H_9NO_2$ | $C_8H_9NO_2$ | $C_8H_9NO_2$ | $C_8H_9NO_2$ | $C_8H_9NO_2$ |
| $M_r$ | 151.16 | 151.16 | 151.16 | 151.16 | 151.16 | 151.16 | 151.16 |
| Cell setting, space group | Monoclinic, $P2_1/c$ | Monoclinic, $P2_1/c$ | Monoclinic, $P2_1/c$ | Monoclinic, $P2_1/c$ | Monoclinic, $P2_1/c$ | Monoclinic, $P2_1/c$ | Monoclinic, $P2_1/c$ |
| Temperature (K) | 298 | 298 | 298 | 298 | 298 | 298 | 298 |
| $a$, $b$, $c$ (Å) | 13.249 (4), 3.9513 (11), 14.402 (4) | 12.998 (3), 3.6988 (5), 13.9167 (16) | 12.941 (4), 3.6146 (5), 13.7188 (17) | 12.878 (4), 3.5363 (5), 13.5218 (16) | 12.831 (3), 3.5096 (4), 13.4462 (13) | 12.766 (7), 3.4872 (9), 13.382 (3) | 12.750 (4), 3.4482 (6), 13.2910 (18) |
| β (°) | 90.324 (4) | 90.99 (2) | 91.47 (2) | 91.88 (2) | 92.10 (2) | 92.27 (4) | 92.45 (2) |
| $V$ (Å$^3$) | 754.0 (4) | 669.0 (2) | 641.5 (2) | 615.5 (2) | 605.11 (16) | 595.2 (4) | 583.8 (2) |
| $Z$ | 4 | 4 | 4 | 4 | 4 | 4 | 4 |
| $D_x$ (Mg m$^{-3}$) | 1.332 | 1.501 | 1.565 | 1.631 | 1.659 | 1.687 | 1.720 |
| Data collection | | | | | | | |
| No. of measured, independent and observed ($I$ > 2.00u($I$)) reflections | 6640, 1786, 627 | 6638, 878, 502 | 6282, 822, 517 | 8856, 1402, 654 | 8863, 1415, 618 | 8106, 1373, 673 | 7902, 1281, 623 |
| $R_{int}$ | 0.041 | 0.233 | 0.157 | 0.199 | 0.271 | 0.222 | 0.242 |
| | | | | | | | |
| Refinement | | | | | | | |
| $R[F^2 > 2\sigma(F^2)]$, $wR(F^2)$, $S$ | 0.049, 0.131, 0.69 | 0.076, 0.212, 1.02 | 0.068, 0.196, 1.02 | 0.062, 0.195, 1.00 | 0.076, 0.240, 0.96 | 0.099, 0.318, 0.93 | 0.059, 0.174, 1.02 |
| No. of reflections | 1786 reflections | 876 reflections | 818 reflections | 1395 reflections | 1404 reflections | 1371 reflections | 1267 reflections |
| No. of parameters | 106 | 106 | 106 | 107 | 106 | 107 | 106 |
| $\Delta\rho_{max}$, $\Delta\rho_{min}$ (e Å$^{-3}$) | 0.14, –0.17 | 0.22, –0.23 | 0.32, –0.19 | 0.20, –0.20 | 0.23, –0.32 | 0.44, –0.38 | 0.18, –0.22 |
| Completeness to 0.83 Å | 100% | 46.4% | 45.3% | 45.5% | 46.3% | 46.4% | 43.9% |

(b) Crystallographic data for 3-methylsalicylaldoxime at increasing pressures.

| | **Ambient** | **1.4 GPa** | **2.7 GPa** | **4.4 GPa** | **5.3 GPa** | **6.0 GPa** |
|---|---|---|---|---|---|---|
| Crystal data | | | | | | |
| Chemical formula | $C_8H_9NO_3$ | $C_8H_9NO_3$ | $C_8H_9NO_3$ | $C_8H_9NO_3$ | $C_8H_9NO_3$ | $C_8H_9NO_3$ |
| $M_r$ | 167.16 | 167.16 | 167.16 | 167.16 | 167.16 | 167.16 |
| Cell setting, space group | Orthorhombic, *Pbca* | Orthorhombic, *Pbca* | Orthorhombic, *Pbca* | Orthorhombic, *Pbca* | Orthorhombic, *Pbca* | Orthorhombic, *Pbca* |
| Temperature (K) | 298 | 298 | 298 | 298 | 298 | 298 |
| *a*, *b*, *c* (Å) | 13.9108 (5), 7.1936 (3), 15.6965 (6) | 13.0765 (5), 7.0982 (4), 15.2455 (5) | 12.5814 (4), 7.0265 (4), 15.0188 (4) | 12.3113 (5), 6.9800 (4), 14.8947 (5) | 12.1340 (13), 6.9421 (11), 14.8065 (13) | 12.0702 (5), 6.9200 (5), 14.7703 (5) |
| $V$ (Å$^3$) | 1570.73 (11) | 1415.08 (11) | 1327.71 (9) | 1279.94 (10) | 1247.2 (3) | 1233.70 (11) |
| $Z$ | 8 | 8 | 8 | 8 | 8 | 8 |
| $D_x$ (Mg m$^{-3}$) | 1.414 | 1.569 | 1.672 | 1.735 | 1.780 | 1.800 |
| | | | | | | |
| Data collection | | | | | | |
| No. of measured, independent and observed ($I$ > 2.00u($I$)) reflections | 17158, 1615, 793 | 12848, 1160, 733 | 12227, 1090, 743 | 12201, 1425, 890 | 11069, 1033, 737 | 11243, 1022, 693 |
| $R_{int}$ | 0.027 | 0.117 | 0.106 | 0.110 | 0.111 | 0.097 |
| | | | | | | |
| Refinement | | | | | | |
| $R[F^2 > 2\sigma(F^2)]$, $wR(F^2)$, $S$ | 0.030, 0.126, 1.13 | 0.046, 0.153, 0.94 | 0.041, 0.119, 0.90 | 0.049, 0.162, 0.87 | 0.048, 0.144, 0.85 | 0.042, 0.111, 0.90 |
| No. of reflections | 1615 reflections | 1155 reflections | 1087 reflections | 1424 reflections | 1029 reflections | 1022 reflections |
| No. of parameters | 115 | 116 | 115 | 115 | 116 | 115 |
| $\Delta\rho_{max}$, $\Delta\rho_{min}$ (e Å$^{-3}$) | 0.16, –0.12 | 0.15, –0.17 | 0.15, –0.18 | 0.25, –0.19 | 0.24, –0.24 | 0.20, –0.17 |
| Completeness to 0.83 Å | 100% | 80.8% | 80.6% | 79.8% | 81.3% | 80.9% |

(c) Crystallographic data for 3-methoxysalicylaldoxime at increasing pressures.

| | **Ambient** | **0.2 GPa** | **1.0 GPa** | **2.3 GPa** | **3.4 GPa** | **4.6 GPa** | **6.2 GPa** |
|---|---|---|---|---|---|---|---|
| Crystal data | | | | | | | |
| Chemical formula | $C_{11}H_{15}NO_2$ | $C_{11}H_{15}NO_2$ | $C_{11}H_{15}NO_2$ | $C_{11}H_{15}NO_2$ | $C_{11}H_{15}NO_2$ | $C_{11}H_{15}NO_2$ | $C_{11}H_{15}NO_2$ |
| $M_r$ | 193.25 | 193.25 | 193.25 | 193.25 | 193.25 | 193.25 | 193.25 |
| Cell setting, space group | Triclinic, *P*-1 | Triclinic, *P*-1 | Monoclinic, *I*2/*a* | Monoclinic, *I*2/*a* | Monoclinic, *I*2/*a* | Monoclinic, *I*2/*a* | Monoclinic, *I*2/*a* |
| Temperature (K) | 298 | 298 | 298 | 298 | 298 | 298 | 298 |
| *a*, *b*, *c* (Å) | 6.6132 (3), 13.1087 (6), 13.6382 (6) | 6.5597 (7), 12.8532 (9), 13.479 (2) | 14.811 (3), 6.4564 (7), 19.759 (4) | 14.5745 (13), 6.3779 (4), 19.0922 (18) | 14.3941 (14), 6.3329 (4), 18.7250 (19) | 14.271 (4), 6.3030 (9), 18.459 (5) | 14.101 (3), 6.2699 (6), 18.158 (3) |
| α, β, γ (°) | 68.762 (3), 76.739 (3), 79.733 (3) | 69.311 (10), 76.054 (10), 79.035 (6) | 90, 94.060 (8), 90 | 90, 94.882 (4), 90 | 90, 95.325 (5), 90 | 90, 95.590 (15), 90 | 90, 95.817 (10), 90 |
| $V$ (Å$^3$) | 1066.71 (9) | 1024.9 (2) | 1884.7 (5) | 1768.3 (3) | 1699.5 (3) | 1652.5 (7) | 1597.1 (4) |
| $Z$ | 4 | 4 | 8 | 8 | 8 | 8 | 8 |
| $D_x$ (Mg m$^{-3}$) | 1.203 | 1.252 | 1.362 | 1.452 | 1.510 | 1.553 | 1.607 |
| | | | | | | | |
| Data collection | | | | | | | |
| No. of measured, independent and observed ($I$ > 2.00u($I$)) reflections | 23029, 4351, 2393 | 8650, 1697, 875 | 8727, 1163, 630 | 8098, 1055, 628 | 7914, 979, 637 | 7728, 920, 569 | 7429, 791, 510 |
| $R_{int}$ | 0.050 | 0.097 | 0.125 | 0.125 | 0.106 | 0.119 | 0.110 |
| | | | | | | | |
| Refinement | | | | | | | |
| $R[F^2 > 2\sigma(F^2)]$, $wR(F^2)$, $S$ | 0.054, 0.134, 0.85 | 0.062, 0.200, 0.92 | 0.062, 0.206, 0.96 | 0.064, 0.225, 0.98 | 0.056, 0.184, 0.96 | 0.067, 0.239, 0.98 | 0.053, 0.163, 0.95 |
| No. of reflections | 4351 reflections | 1688 reflections | 1163 reflections | 1055 reflections | 979 reflections | 918 reflections | 790 reflections |
| No. of parameters | 265 | 265 | 134 | 134 | 134 | 134 | 134 |
| $\Delta\rho_{max}$, $\Delta\rho_{min}$ (e Å$^{-3}$) | 0.17, –0.15 | 0.12, –0.13 | 0.16, –0.16 | 0.23, –0.26 | 0.18, –0.20 | 0.24, –0.27 | 0.16, –0.17 |
| Completeness to 0.83 Å | 100% | 41.8% | 62.4% | 60.1% | 57.4% | 55.8% | 49.8% |

(d) Crystallographic data for 3-*tert*-butylsalicylaldoxime at increasing pressures.

Crystal structures were visualized using the programs MERCURY[22] and DIAMOND.[23] Analyses were carried out using PLATON,[24] as incorporated in the WinGX suite.[25] Searches of the Cambridge Structural Database[26, 27] utilized the program ConQuest and version 5.27 of the database with updates up to August 2006. Equation-of-state calculations were carried out with EOSFIT.[28]

The numbering schemes used [Scheme 1a-e] are the same for each compound. The oxime group is formed by H1-O1-N2-C3, and the hydroxyl group by O5H5; in the case of the two molecules comprising the asymmetric unit of 3-*tert*-butylsalicylaldoxime-I these labels are augmented by '1' or '2' (O51-H51, O52-H52 *etc*.).

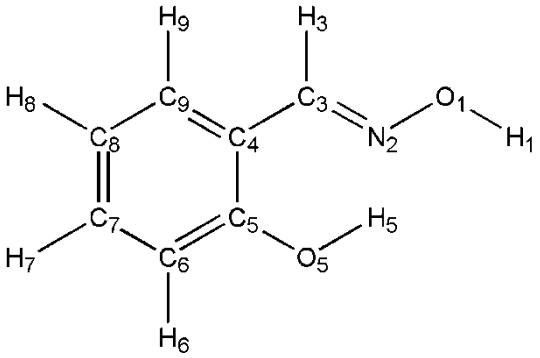


**a**

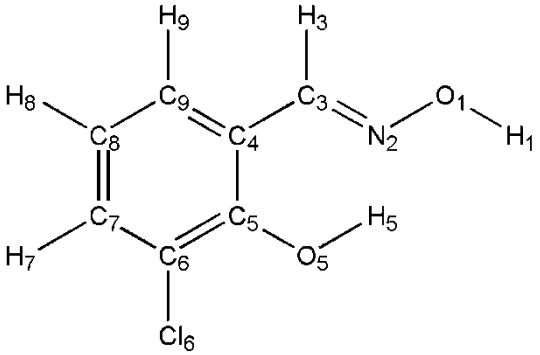


**b**

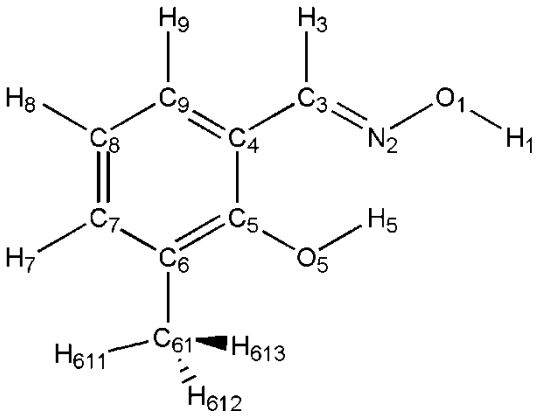


**c**

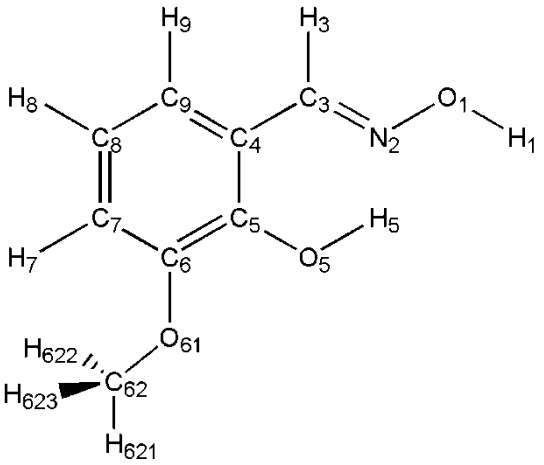


**d**

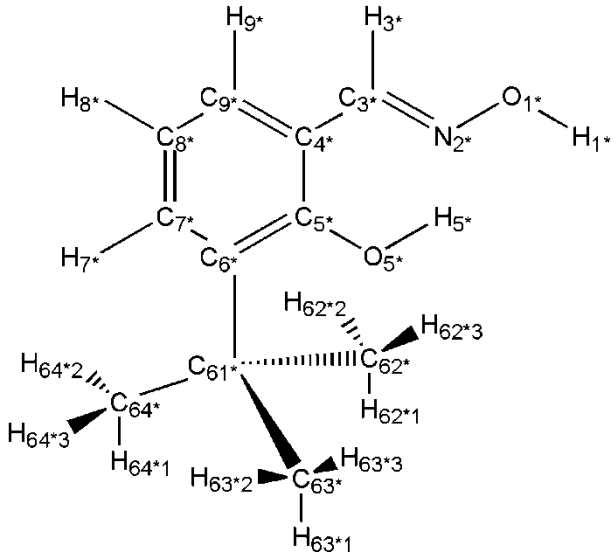


**e**

***Scheme 1.*** Chemical structure diagrams showing atomic numbering schemes for salicylaldoxime (a), 3-chlorosalicylaldoxime (b), 3-methylsalicylaldoxime (c), 3-methoxysalicylaldoxime (d), and 3-*tert*-butylsalicylaldoxime (e).

*PIXEL Calculations*

The final crystal structures obtained were used to calculate the molecular electron density at each pressure by standard quantum chemical methods using the program GAUSSIAN98[29] with the MP2/6-31G** basis set. H-atom distances were set to standard neutron values (C-H = 1.083 Å, OH = 0.983 Å). The electron density model of the molecule was then analysed using the program package OPiX[30, 31] which allows the calculation

of dimer and lattice energies. The output from these calculations yields a total energy and a breakdown into its electrostatic, polarisation, dispersion and repulsion components.[32]

***Results***

*The structures of the substituted salicylaldoximes at ambient pressure*

3-Methyl-, 3-methoxy- and 3-chloro-salicylaldoxime all crystallise with one molecule in the asymmetric unit, while the asymmetric unit of 3-*tert*-butylsalicylaldoxime contains two molecules. Prior to this work only one of the four compounds studied, 3-methoxysalicylaldoxime, had been crystallographically characterized.[33] Each of these structures exhibits intramolecular phenolic O5*-H5*…N2* hydrogen bonds and intermolecular oximic O1*-H1*…O5* hydrogen bonds (where * = 1 or 2 for 3-*tert*-butylsalicylaldoxime). The latter form a dimer motif across an inversion centre (Figure 1) in a similar manner to that seen in salicylaldoxime[9] for which the graph-set descriptor is $R_4^4(10)$.[34]

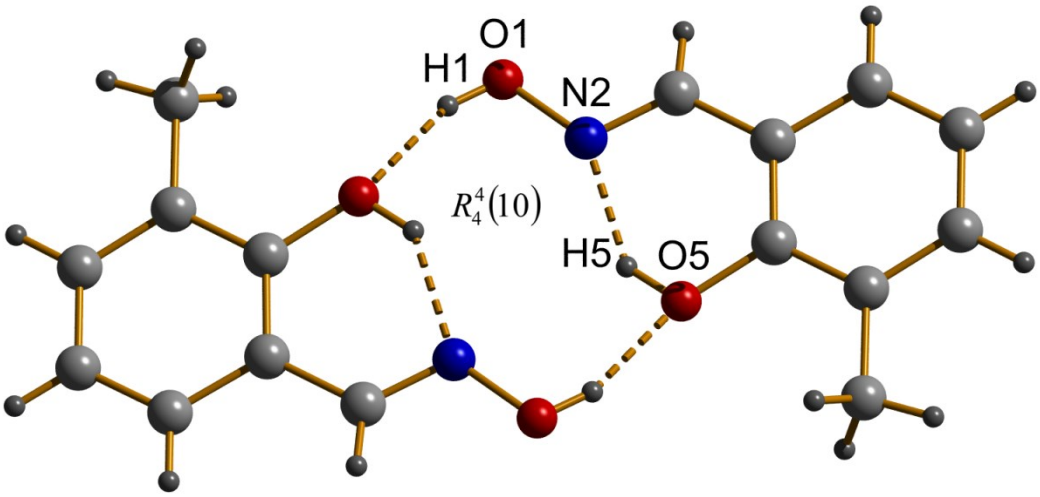


***Figure 1.*** The hydrogen-bonded $R_4^4(10)$ ring motif across an inversion centre in the structure of 3-methylsalicylaldoxime at ambient pressure. The colour scheme is red: oxygen, blue: nitrogen, light-grey: carbon and dark-grey: hydrogen.

The salicylaldoxime molecule is essentially planar in each structure, though the perpendicular distance between the two molecules of the $R_4^4(10)$ dimer varies. The distances between the least squares planes of the two hydrogen bonded salicylaldoxime molecules are 0.967, 1.122, 0.836, 0.730 and 0.404 Å for 3-

chlorosalicylaldoxime, 3-methylsalicylaldoxime, 3-methoxysalicylaldoxime and the two different dimers in 3-*tert*-butylsalicylaldoxime, respectively.

The structures of 3-chlorosalicylaldoxime and 3-methylsalicylaldoxime have similar cell dimensions and are almost isomorphous. The $R_4^4(10)$ dimers are stacked *via* cell-translations along [010] to form π-π contacts between phenyl groups [stacking distance = 3.464 (1) Å and 3.533 (2) Å for 3-chloro and 3-methylsalicylaldoxime, respectively], which connect the dimers into ribbons running in the direction of the *b*-axis. The ribbons are then held together by C3H3…O1 interactions [C3…O1 = 3.583 (3) Å and 3.722 (3) Å for 3-chloro and 3-methylsalicylaldoxime respectively] to form slabs in the (100) plane. In the structure of 3-methylsalicylaldoxime the slabs interact only through weak van der Waals contacts and are arranged so that H…H contacts are approximately equidistant (Figure 2a). The 3-chlorosalicylaldoxime structure, however, shows a shifting of the slabs with respect to the methyl form in order to optimise the CH…Cl contacts in the structure, two of which are formed between the slabs (Figure 2b). The packing of the 3-chloro form includes three CH…Cl intermolecular interactions of similar length [C…Cl = 3.626 (2), 3.661 (2), 3.699 (2) Å] and two slightly longer CH…Cl contacts [C…Cl = 4.027 (2) and 4.200 (2) Å].

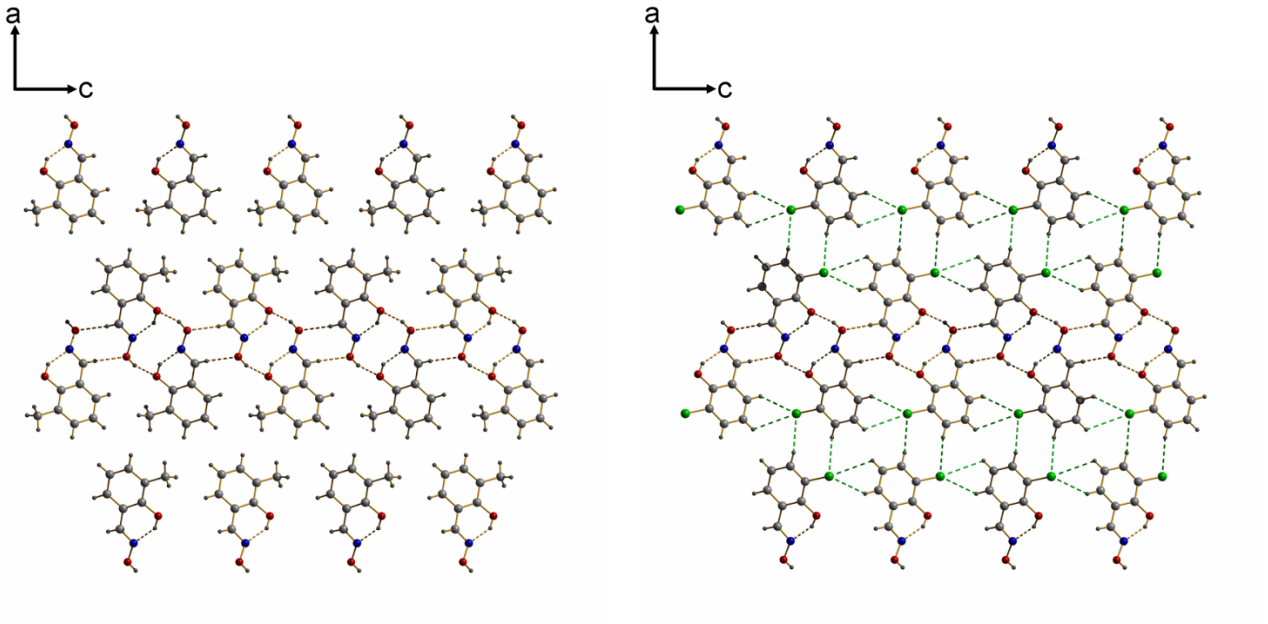


***Figure 2.*** The structure of 3-methylsalicylaldoxime (a) and 3-chlorosalicylaldoxime (b) at ambient pressure as viewed along the *b*-axis. This view illustrates the similarity and differences in the formation of slabs in these crystal structures. Hydrogen bonds are shown as dashed yellow lines and close CH…Cl contacts are shown as dashed green lines. The colour scheme is the same as in Fig. 1 with the addition of green: chlorine.

3-Methoxysalicylaldoxime also contains a π-π stacking motif between phenyl rings. In this structure the stacking molecules are related by an inversion centre, and each molecule interacts with only one other in this fashion, rather than in the infinite stack arrangement seen in salicylaldoxime, 3-chlorosalicylaldoxime and 3-methylsalicylaldoxime. The other side of the phenyl ring forms a CH…π interaction with the phenyl hydrogen atoms of an adjacent molecule; repetition of this motif generates a herringbone-like pattern (Figure 3). The hydrogen bonded dimer and the stacking motif combine to form ribbons which run along the *b*-axis; the ribbons are then connected *via* the CH…π interactions into slabs in the (001) plane. The slabs then interact with each other through C3H3…O1 interactions [C3…O1 = 3.368 (3) Å].

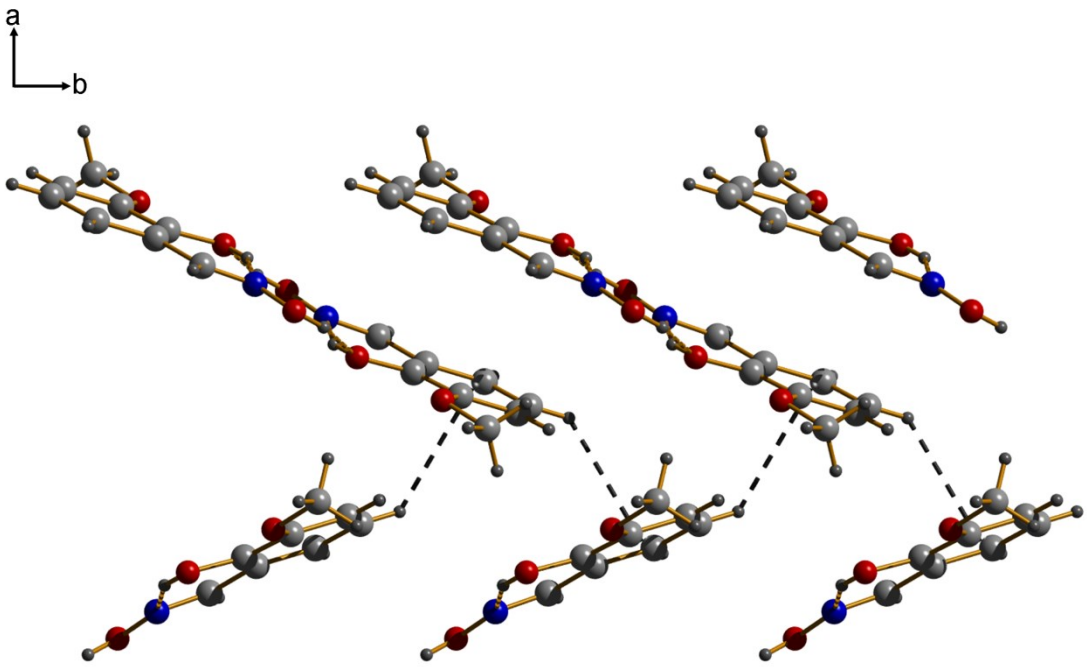


***Figure 3.*** The structure of 3-methoxysalicylaldoxime at ambient pressure as viewed along the *c*-axis. This view illustrates the stacking interactions between the dimer units and the CH…π interactions (shown as dashed grey lines) in the structure which form a herringbone-like pattern. The colour scheme is the same as in Fig. 1.

The structure of 3-*tert*-butylsalicylaldoxime contains two molecules in the asymmetric unit and has the space group *P*-1. Each symmetry-independent molecule forms a hydrogen bonded dimer across an inversion centre, and exhibits a π-π stacking interaction with a molecule related by another inversion centre (Figure 4). Like the 3-methoxy substituted form, 3-*tert*-butylsalicylaldoxime only forms a stacking interaction on one side of the phenyl ring and is involved in a CH…π interaction on the other side, in this case with the *tert*-butyl group of the other molecule in the asymmetric unit. The hydrogen bonded dimer and stacking interactions again form

ribbons, which in this case run along the *a*-axis, and the ribbons are then connected to each other *via* the CH…π interactions to form slabs in the (0-11) plane. These slabs interact with each other through long CH…O interactions [C31…O12 = 3.629 (3) Å and C32…O11 = 3.611 (3) Å].

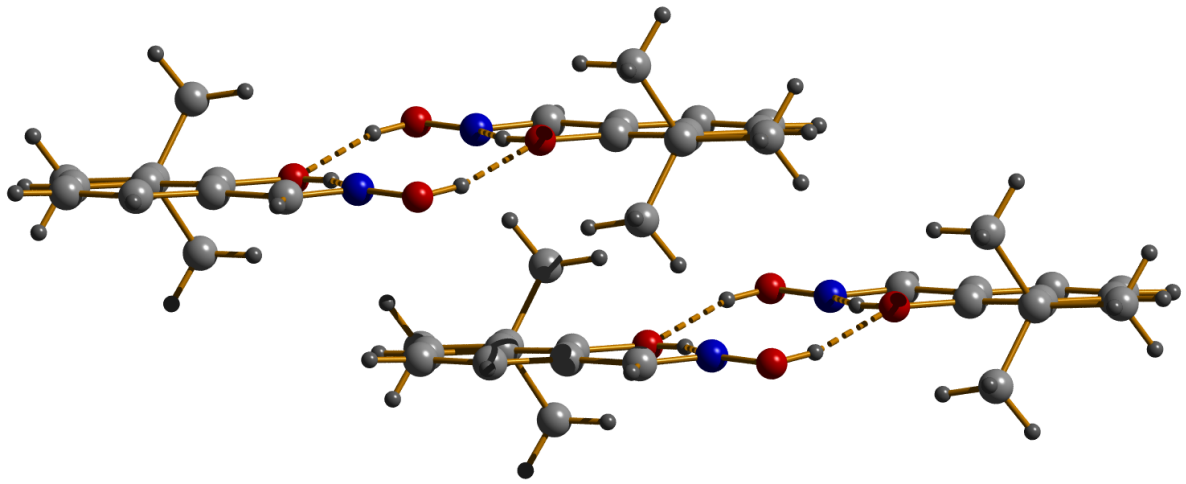

***Figure 4.*** The structure of 3-*tert*-butylsalicylaldoxime-I at ambient pressure showing the π-π stacking interaction between two hydrogen-bonded dimers for one of the crystallographically independent molecules. The colour scheme is the same as in Fig. 1.

*The phase transition in 3-tert-butylsalicylaldoxime*

The phase transition from 3-*tert*-butylsalicylaldoxime-I to 3-*tert*-butylsalicylaldoxime-II occurs between 0.2 and 1.0 GPa and proceeds from one single crystal to another single crystal. The space group changes from *P*-1 to *I*2/*a*, the two crystallographically independent molecules of the triclinic phase becoming equivalent after the phase transition. The non-covalent interaction motifs of the structure remain essentially the same through the phase transition with the structure retaining the $R_4^4(10)$ hydrogen bonded dimer motif and the π-π stacking. These two intermolecular interactions form ribbons as in the ambient phase, but these now run along the crystallographic *b*-axis. The independent CH…π interactions of the triclinic phase are averaged with the distances from the closest hydrogen to the plane of the phenyl ring changing from 2.79 and 2.63 Å in the 0.2 GPa phase I structure to 2.69 Å in the 1.0 GPa phase II structure. The ribbons are connected through these CH…π contacts in the high pressure structure to form slabs in the (100) plane. The C3H3…O1 interactions between the slabs persist through the phase transition, though the C…O distances are shorter [C3…O1 = 3.432 (7) Å].

*The response to pressure of the substituted salicylaldoximes*

The effect of pressure on the substituted oximes is anisotropic, the changes in unit cell dimensions with pressure, are given in Tables 1(a) to (d). The bulk moduli ($K_0$) calculated using a Birch-Murnaghan equation-of-state[35, 36] are 12.1(4), 12.2(5), 14.2(6) and 15.6(6) GPa respectively for the chloro-, methyl-, methoxy- and *t*-butyl derivatives, compared to the value of 13.3 (4) GPa calculated for salicylaldoxime itself. The variation in unit cell volumes is therefore fairly consistent across this series of compounds. Molecular solids generally have $K_0 < 30$ GPa and a useful comparison can be made from the following $K_0$ values (GPa): $Ru_3(CO)_{12}$ 6.6, NaCl 25, quartz 37, ceramics 50–300 and diamond 440.[37]

The changes in non-covalent interaction geometries with pressure for the series of compounds are shown in Table 2. Consistently across the series of compounds the least compressible interaction is the intramolecular phenolic OH…N hydrogen bonding interaction (O…N distance decreases by between 1.5 and 2.2 %). The other conventional hydrogen bond in the structures, the oximic intermolecular OH…O interaction, is more compressible (the O…O distance decreases by between 4.7 and 6.5 %). These hydrogen bonding interactions retain roughly the same donor-hydrogen-acceptor angles with compression, so the conformation of the hydrogen bonding ring in each structure remains essentially unchanged. The deviation from planarity of the $R_4^4(10)$ rings is also insensitive to pressure throughout the series (e.g. the interplanar distance in 3-methylsalicylaldoxime is 1.122 Å at ambient pressure and 1.149 at 5.6 GPa; corresponding data for the 3-chloro derivative are 0.967 and 1.026 Å at 5 GPa).

| Pressure/GPa | 0.0 | 1.6 | 2.4 | 3.4 | 5.0 |
|---|---|---|---|---|---|
| **O5H5..N2**[i] | | | | | |
| H5..N2 | 1.85 | 1.80 | 1.79 | 1.77 | 1.79 |
| O5..N2 | 2.589(2) | 2.562(13) | 2.550(11) | 2.550(16) | 2.538(15) |
| <O5H5N2 | 150(2) | 149 | 153 | 152 | 146 |
| **O1H1..O5**[ii] | | | | | |
| H1..O5 O1..O5 | 2.07 | 1.97 | 1.91 | 1.94 | 1.88 |
| <O1H1O5 | 2.783(2) | 2.731(10) | 2.709(8) | 2.692(12) | 2.653(11) |
| | 156(2) | 149 | 152 | 147 | 151 |
| **π-π**[iii] | | | | | |
| plane-plane | 3.464(1) | 3.242(3) | 3.191(3) | 3.122(4) | 3.055(4) |
| offset | 1.761(1) | 1.701(2) | 1.656(3) | 1.645(3) | 1.586(4) |

**Symmetry Operators:**

| | |
|---|---|
| i | *x*,*y*,*z* |
| ii | -*x*,-*y*,-*z* |
| iii | *x*,-1+*y*,*z* |

***Table 2.*** ↑ (a) Non-covalent interaction parameters in 3-chlorosalicylaldoxime. Distances are in Å, and angles in °

| Pressure/GPa | 0.0 | 1.3 | 2.2 | 3.5 | 4.2 | 4.9 | 5.6 |
|---|---|---|---|---|---|---|---|
| **O5H5..N2**[i] | | | | | | | |
| H5..N2 | 1.85 | 1.80 | 1.86 | 1.79 | 1.86 | 1.80 | 1.82 |
| O5..N2 | 2.608(2) | 2.597(7) | 2.585(7) | 2.573(6) | 2.576(6) | 2.572(7) | 2.570(6) |
| <O5H5N2 | 143(2) | 151 | 138 | 144 | 137 | 147 | 145 |
| **O1H1..O5**[ii] | | | | | | | |
| H1..O5 O1..O5 | 2.06 | 2.03 | 1.94 | 1.80 | 1.87 | 1.88 | 1.77 |
| <O1H1O5 | 2.806(3) | 2.750(6) | 2.732(5) | 2.694(4) | 2.684(5) | 2.675(6) | 2.658(4) |
| | 153(3) | 141 | 156 | 168 | 155 | 150 | 156 |
| **π-π**[iii] | | | | | | | |
| plane-plane | 3.533(2) | 3.314(2) | 3.238(2) | 3.167(2) | 3.139(2) | 3.117(2) | 3.080(2) |
| offset | 1.769(2) | 1.643(2) | 1.607(2) | 1.573(2) | 1.571(2) | 1.563(2) | 1.550(2) |

**Symmetry Operators:**

| | |
|---|---|
| i | *x*,*y*,*z* |
| ii | -*x*,-*y*,-*z* |
| iii | *x*,-1+*y*,*z* |

↑ (b) Non-covalent interaction parameters in 3-methylsalicylaldoxime. Distances are in Å, and angles in °

| Pressure/GPa | 0.0 | 1.4 | 2.7 | 4.4 | 5.3 | 6.0 |
|---|---|---|---|---|---|---|
| **O5H5..N2**[i] | | | | | | |
| H5..N2 | 1.79 | 1.81 | 1.77 | 1.76 | 1.81 | 1.85 |
| O5..N2 | 2.586(3) | 2.567(3) | 2.552(3) | 2.542(2) | 2.536(2) | 2.534(3) |
| <O5H5N2 | 151(3) | 144 | 150 | 150 | 150 | 143 |
| **O1H1..O5**[ii] | | | | | | |
| H1..O5 O1..O5 | 1.88 | 1.90 | 1.79 | 1.81 | 1.77 | 1.77 |
| <O1H1O5 | 2.707(2) | 2.655(3) | 2.617(3) | 2.598(3) | 2.581(3) | 2.578(3) |
| | 155(3) | 152 | 158 | 149 | 156 | 149 |
| **π-π**[iii] | | | | | | |
| plane-plane | 3.429(2) | 3.270(2) | 3.165(2) | 3.102(2) | 3.058(2) | 3.046(2) |
| offset | 1.820(1) | 1.655(1) | 1.577(1) | 1.548(1) | 1.536(1) | 1.524(1) |

**Symmetry Operators:**

| | |
|---|---|
| i | *x*,*y*,*z* |
| ii | -*x*,-*y*,-*z* |
| iii | 1-*x*,1-*y*,1-*z* |

↑ (c) Non-covalent interaction parameters in 3-methoxysalicylaldoxime. Distances are in Å, and angles in °

| Pressure/GPa | 0.0 | 0.2 |
|---|---|---|
| **O51H51..N21**[i] | | |
| H51..N21 | 1.81 | 1.85 |
| O51..N21 | 2.597(3) | 2.620(14) |
| <O51H51N21 | 150(2) | 145 |
| **O11H11..O51**[ii] | | |
| H11..O51 O11..O51 | 2.00 | 1.96 |
| <O11H11O51 | 2.811(3) | 2.769(8) |
| | 156(3) | 155 |
| **O52H52..N22**[i] | | |
| H52..N22 | 1.84 | 1.89 |
| O52..N22 | 2.599(2) | 2.614(18) |
| <O52H52N22 | 148(2) | 143 |
| **O12H12..O52**[iii] | | |
| H12..O52 O12..O52 | 1.99 | 2.00 |
| <O12H12O52 | 2.827(3) | 2.813(8) |
| | 164(4) | 157 |
| **π-π**[iv] | | |
| plane-plane | 3.371(2) | 3.314(5) |
| offset | 3.768(2) | 3.745(5) |
| **π-π**[v] | | |
| plane-plane | 3.696(2) | 3.612(6) |
| offset | 3.309(2) | 3.249(5) |

**Symmetry Operators:**

| | |
|---|---|
| i | *x*,*y*,*z* |
| ii | 2-*x*,-*y*,-*z* |
| iii | 1-*x*,1-*y*,1-*z* |
| iv | 1-*x*,-*y*,-*z* |
| v | -*x*,1-*y*,1-*z* |

↑ (d) Non-covalent interaction parameters in 3-*tert*-butylsalicylaldoxime-I. Distances are in Å, and angles in °

| Pressure/GPa | 1.0 | 2.3 | 3.4 | 4.6 | 6.2 |
|---|---|---|---|---|---|
| **O5H5..N2**[i] | | | | | |
| H5..N2 | 1.80 | 1.84 | 1.80 | 1.80 | 1.76 |
| O5..N2 | 2.569(6) | 2.578(6) | 2.586(6) | 2.551(7) | 2.541(9) |
| <O5H5N2 | 148(5) | 145 | 146 | 145 | 148 |
| **O1H1..O5**[ii] | | | | | |
| H1..O5 O1..O5 | 1.94 | 1.96 | 1.93 | 1.90 | 1.90 |
| <O1H1O5 | 2.763(5) | 2.723(5) | 2.694(5) | 2.677(6) | 2.653(6) |
| | 157(3) | 152 | 153 | 148 | 148 |
| **π-π**[iii] | | | | | |
| plane-plane | 3.308(3) | 3.192(3) | 3.114(3) | 3.065(4) | 3.011(3) |
| offset | 3.382(3) | 3.332(3) | 3.302(3) | 3.274(4) | 3.239(3) |

**Symmetry Operators:**

| | |
|---|---|
| i | *x*,*y*,*z* |
| ii | 0.5-*x*,0.5-*y*,0.5-*z* |
| iii | 0.5-*x*,1.5-*y*,0.5-*z* |

↑ (e) Non-covalent interaction parameters in 3-*tert*-butylsalicylaldoxime-II. Distances are in Å, and angles in °

The most compressible of the three non-covalent interactions in the structures is the π-π stacking interaction, which can be described by the perpendicular distance between the least-squares mean plane of one phenyl ring to the centroid of another (stacking distances decrease by between 11.2 and 14.9 %).

***Discussion***

*The effect of pressure on cavity size in the substituted salicylaldoximes*

The size of the intermolecular cavity, which occurs within the hydrogen bonded ring motif, can be studied by measuring the mean distance from the metal to the donor atoms of the ligands (*i.e.* O5, N2) to the centroid of the dimer. This distance was shown[9] to decrease approximately linearly in the case of salicylaldoxime-I within the pressure range of 0-5.3 GPa. Figure 5 shows a graph of the cavity size as a function of pressure as determined in this study. We can see that the cavity sizes decrease for all the compounds and, with the exception of the *tert*-butyl phase I (from 0 – 1 GPa in Figure 5), with very similar gradients.

The cavity size at ambient pressure is found to be markedly dependent on the nature of the 3-substituent which is *ortho* to the phenolic OH group (X in Scheme 2). The trend appears to be related to the ability of the substituent to accept a hydrogen bond. If it has a lone pair capable of accepting a hydrogen bond, the oximic hydrogen can in principle form an asymmetric bifurcated hydrogen bond, encouraging the molecules to approach each other more closely (see Scheme 2). On this basis the 3MeO- and 3Cl- are expected and are found to have the smallest cavity radii (Table 3) Conversely when the 3-substituent is bulky it will weaken the oximic H to phenolic O hydrogen bonding and a larger cavity will result, as in the 3-*t*-Bu compound (see Table 3).

| **3-Substituent** | **OMe** | **Cl** | **H** | **Me** | **$^{t}$Bu** |
|---|---|---|---|---|---|
| Cavity size at ambient pressure/Å | 1.9492(19) | 1.9837(12) | 2.0048(15) | 2.0237(18) | 2.0367(19) |
| $E_{coul}$ / kJmol$^{-1}$ | -4.8 | -0.5 | 0 | +0.2 | +2.1 |
| $E_{rep}$ / kJmol$^{-1}$ | -0.4 | 0.0 | 0 | +0.6 | +6.2 |
| $E_{pol}$ / kJmol$^{-1}$ | -1.0 | -1.0 | 0 | -0.8 | -2.7 |
| $E_{disp}$ / kJmol$^{-1}$ | -0.8 | -1.5 | 0 | -1.5 | -5.8 |
| $E_{TOTAL}$ / kJmol$^{-1}$ | -7.0 | -3.0 | 0 | -1.5 | -0.2 |

***Table 3.*** Ambient-pressure cavity sizes and differences in energy for the hydrogen bonded dimers in the substituted oximes structures with and without the substituent. The values are calculated for each dimer and then for the same geometry but with the substituent replaced by an H atom. The energies of the components in the salicylaldoxime-I dimer contact are -37.1, -7.8, 35.0, -15.0 and -25.0 kJ $mol^{-1}$ for the coulombic, dispersion, repulsion, polarisation and total energies respectively. Energies are in kJ $mol^{-1}$. The cavity size for the tBu derivative is the average for the two molecules comprising the asymmetric unit.

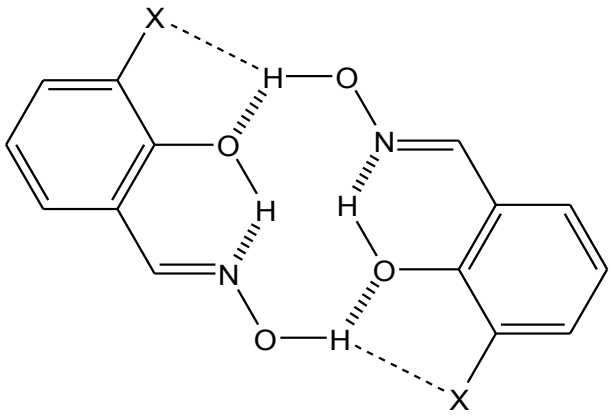


***Scheme 2.*** Hydrogen bonding within the pseudomacrocyclic dimer showing potential interactions with the 3-substituent (X).

In order to test this theory a set of energy calculations were performed using the geometry of the crystal structures and the PIXEL method,[32, 38] which models intermolecular interaction energies in terms of Coulombic, polarization and dispersive-repulsion contributions. PIXEL energies were calculated first for each dimer and then for the same geometry but with the substituent replaced by an H atom. The differences are reported in Table 3.

The Coulombic term favours the association of the dimer when the 3MeO- and 3Cl- are present (Table 3) which is consistent with their H-bond acceptor properties whilst it disfavours association for the 3Me- and the 3-*t*-Bu substituted compounds. A large repulsion term ($E_{rep}$) is seen for the $^{t}$Bu-substituted ligand, which may explain both its large hole size and poor extractive efficacy. However, the method also suggests there is a slightly stronger net attraction between the two halves of the Me and $^{t}$Bu substituted dimers than in the unsubstituted system. Both have large, favourable dispersion terms, $E_{disp}$, due to the number of electrons in the substituents, though it is possible that this term may be over-estimated as it is the most parameterised in the PIXEL formalism.[39]

Figure 5 shows that the relative compressibilities of the hole sizes in the five different compounds are quite similar, no doubt reflecting the similarity of the interactions involved. The relative changes in cavity size (=

cavity size at ambient pressure / cavity size at 5 GPa) are 1.031(4) (Me) and 1.031(6) (Cl) 1.036(3) (H), 1.043(2) (OMe) and 1.054(3) (*t*Bu). Though these data refer to compression of an entire crystal structure, not an isolated dimer, it is noteworthy that the compressibility of the 3-*tert*-butylsalicylaldoxime cavity is greater than the other salicylaldoximes, and the hole size becomes smaller than that of the 3-methyl and unsubstituted compounds at elevated pressure. This is counter-intuitive as the *tert*-butyl group is expected to be sterically repulsive: indeed steric effects have been used to explain the weakness of this ligand in binding $Cu^{2+}$ at ambient pressure.[13]

An important practical consequence of the data presented in Figure 5 is that the combination of varying the nature of the 3-substituent and of changing the pressure can change the $N_2O_2$ cavity radius between 1.87 and 2.04 Å. This range spans the covalent radii of many of the 1st transition series metal dications and should allow the selectivity of metal extraction to be tuned using pressure.

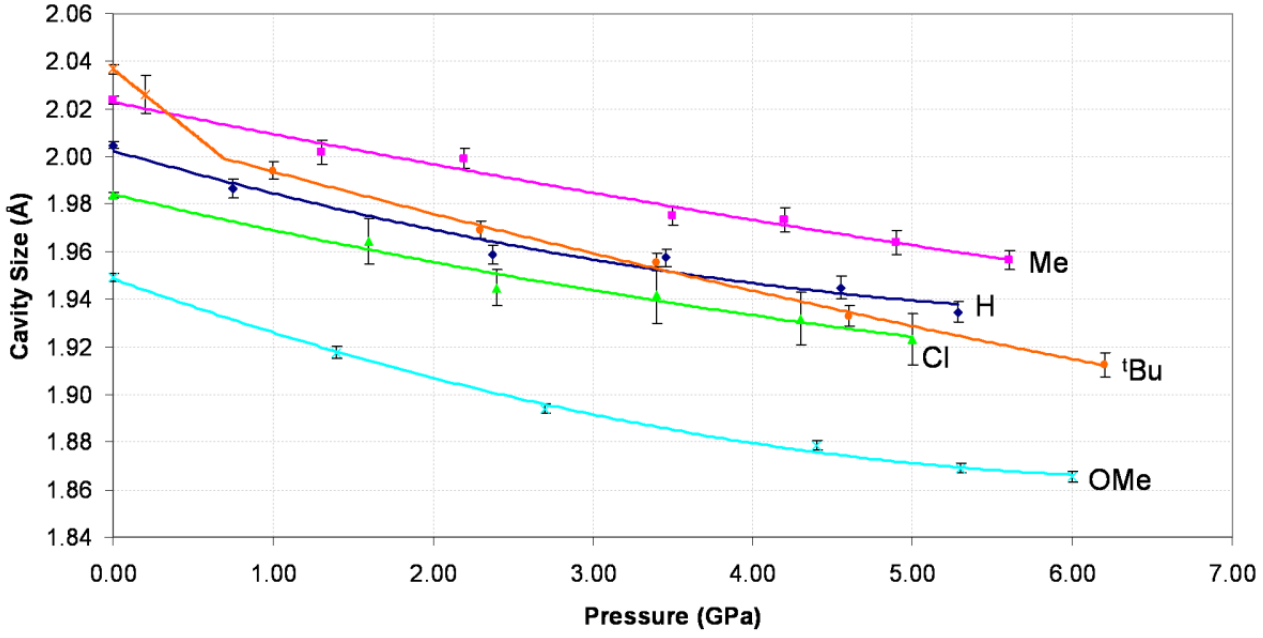


***Figure 5.*** Graph of cavity size (in Å) as a function of pressure (in GPa) for salicylaldoxime (dark blue), 3-chlorosalicylaldoxime (green), 3-methylsalicylaldoxime (pink), 3-methoxysalicylaldoxime (light blue) and 3-*tert*-butylsalicylaldoxime (orange). Cavity size is defined as the mean distance of donor atoms from the centroid of the dimer. Each pressure series (except for tBu) has been fitted with a line of best fit using a polynomial of order 2; these are guides to the eye rather than equations of state. The two phases of 3-*tert*-butylsalicylaldoxime have been plotted separately with a trend line fitted to each set of points, both are coloured orange. The error bars are shown at the 1σ level.

*Analysis of non-covalent interactions under compression*

The effect of pressure on the intermolecular interactions within the substituted salicylaldoximes is non-uniform. There are three main non-covalent interactions which are found in each of the different compounds; the phenolic OH…N intramolecular hydrogen bond, the oximic OH…O intermolecular hydrogen bond and the π-π stacking interaction. The OH…N intramolecular hydrogen bond is the least compressible non-covalent interaction in the structures and is relatively consistent across the series of compounds due to the rigidity of the salicylaldoxime molecular geometry. The oximic OH…O hydrogen bond geometry is not restricted by the covalent bonds of the molecule and thus is considerably more compressible than the intramolecular hydrogen bond. Figure 6 shows a graph of the variation in the donor to acceptor distances for the OH…O hydrogen bond as a function of pressure for each of the compounds. The oximic hydrogen bond in the 3-methoxysalicylaldoxime structure is considerably shorter than the corresponding interaction in the other compounds both at ambient pressure and when compressed. As described above, this is ascribable to the availability of the methoxy oxygen atom as a secondary hydrogen bond acceptor (Figure 7). The shapes of the H, Me, and Cl curves are very similar though, so it would appear that changing the substituent can modify the length of the OH…O interaction and thus the size of the pseudo-macrocyclic cavity at ambient conditions, but doesn't significantly affect the compressibility of the interaction.

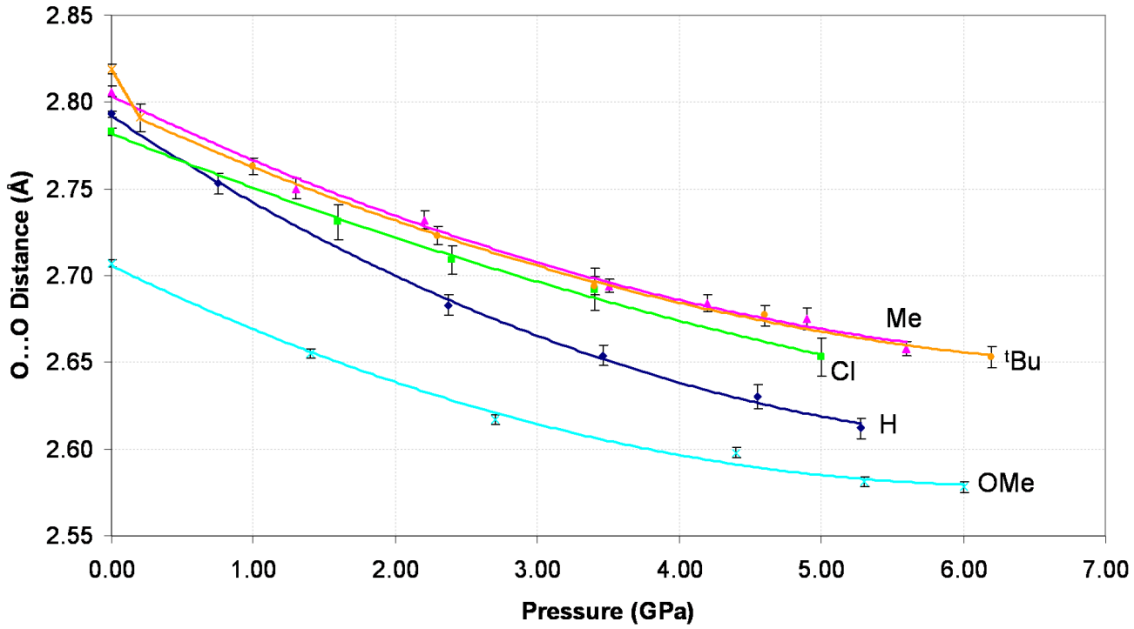


***Figure 6.*** Graph of donor to acceptor distance (in Å) of the oximic OH…O intermolecular interaction as a function of pressure (in GPa) for salicylaldoxime (dark blue), 3-chlorosalicylaldoxime (green), 3-methylsalicylaldoxime (pink), 3-methoxysalicylaldoxime (light blue) and 3-*tert*-butylsalicylaldoxime (orange).

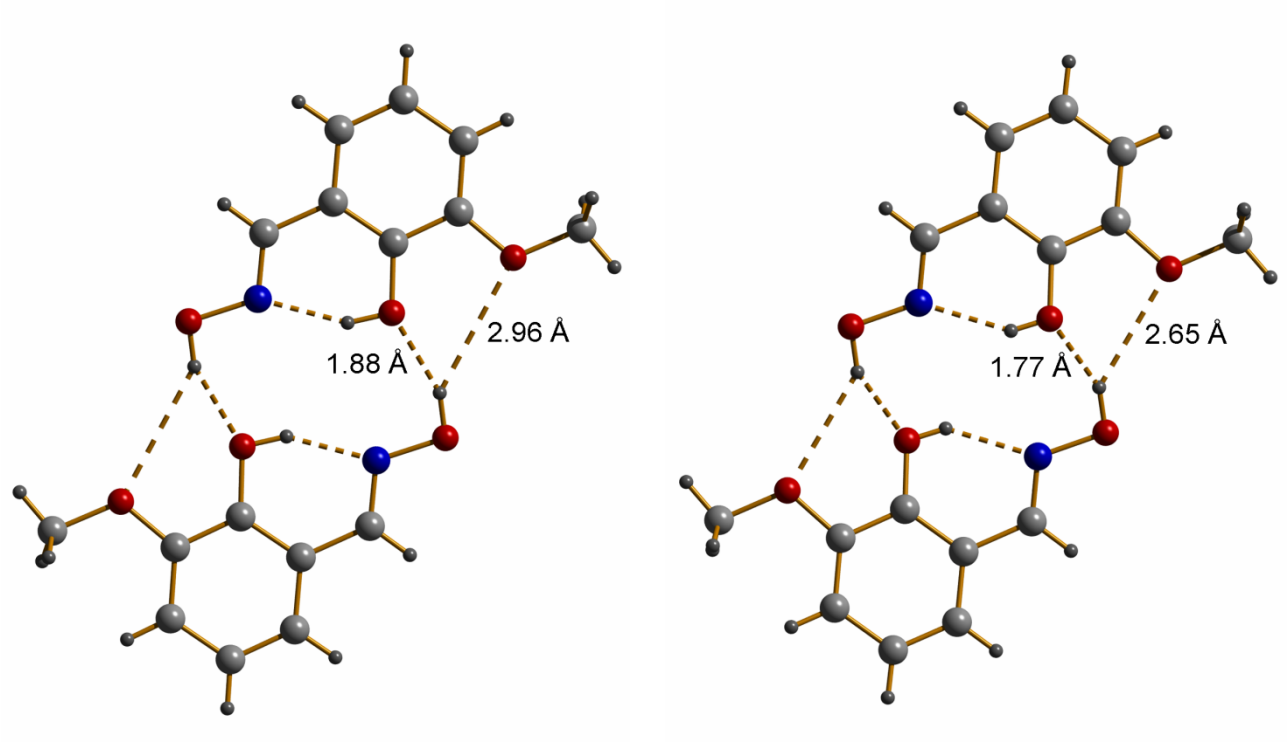


***Figure 7.*** The hydrogen bonded dimer with bifurcated character in 3-methoxysalicylaldoxime at ambient pressure (a) and at 6.0 GPa (b). The distances displayed are H to O distances for O1H1…O5 and O1H1…O61. The colour scheme is the same as in Fig. 1.

The stacking interaction in these structures is seen to be more compressible than the hydrogen bonds but, as PIXEL calculations on the salicylaldoxime compression study showed,[9] the interactions can become very repulsive at shorter distances. This sharp increase in repulsion as the stacking distance reaches its minimum means that the interaction can become important in terms of both anisotropic compression and phase transitions. To analyse the compression of these stacking interactions it is useful to compare them to similar interactions found at ambient conditions. The stacking interaction between phenyl groups can be described using the angle between phenyl ring planes, the perpendicular distance between the groups (stacking distance) and the parallel distance between groups (stacking offset). A search of the CSD was performed for phenyl groups interacting in a stacking configuration with planar angle < 10˚, stacking distance < 4.5 Å, stacking offset < 4.0 Å, 3D coordinates and R-factor < 0.05 in organic-only structures without errors or disorder.

Figure 8 shows a graph of stacking distance against stacking offset for all the interactions found in the CSD. Also shown are the stacking contacts in the five salicylaldoxime compression studies performed to date. This graph shows that the stacking interaction for each compound is at a normal distance at ambient conditions, but as pressure is increased the interactions are compressed to the limits of similar interactions seen at ambient

pressures. The salicylaldoxime crystal structure was seen to undergo a phase transition between 5.3 and 5.9 GPa.[9] This was believed to be caused in part by the stacking interaction reaching the limits of similar interactions found at ambient conditions. The data in Figure 8 suggests that each of the substituted salicylaldoximes studied here may also be close to a phase transition at the highest pressures obtainable in this study.

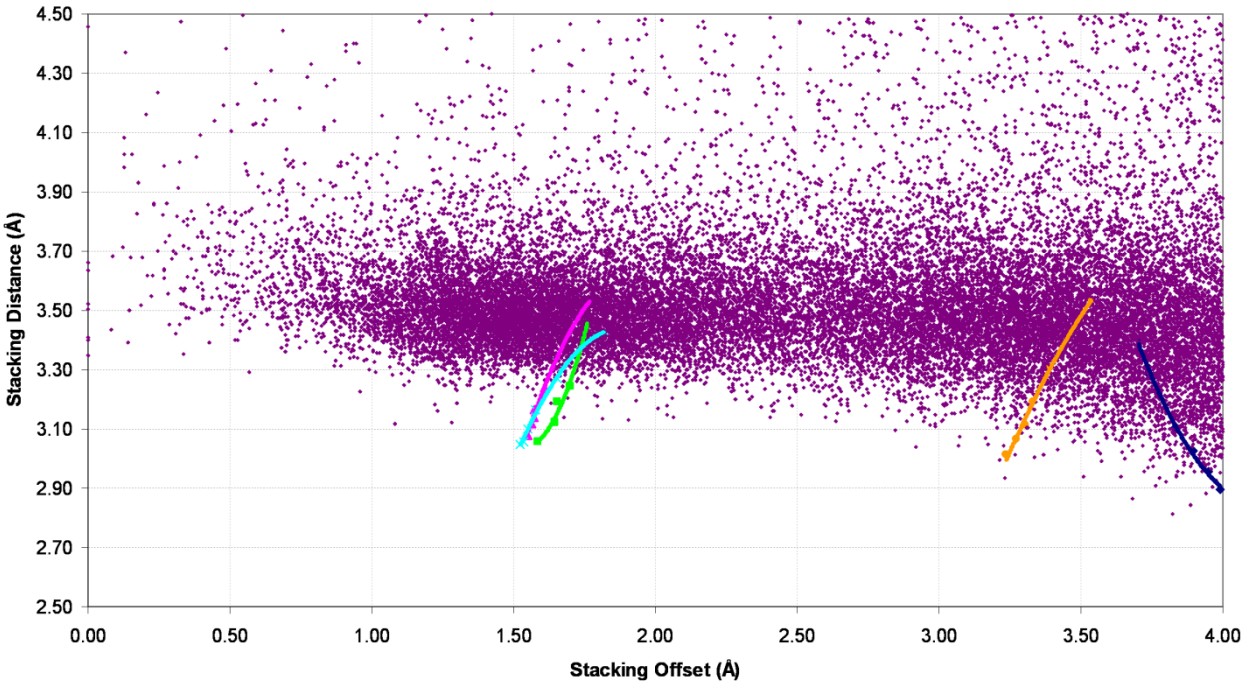


***Figure 8.*** Graph of stacking distance (in Å) against stacking offset (in Å) for phenyl group stacking interactions in the CSD. The five oxime compression studies have also been plotted; salicylaldoxime (dark blue), 3-chlorosalicylaldoxime (green), 3-methylsalicylaldoxime (pink), 3-methoxysalicylaldoxime (light blue) and 3-*tert*-butylsalicylaldoxime (orange).

The range of pressures that were obtained in the experiments described in this paper was limited by the hydrostatic pressure medium, the tungsten gasket and the single crystals themselves. It would be interesting to investigate the phase behaviour of salicylaldoximes at elevated pressures using powder methods.

## *Conclusions*

The crystal structures of salicylaldoxime and the four 3-substitued derivatives (OMe, Cl, Me and $^t$Bu) examined in this study comprise pseudomacrocyclic dimers based on an $R_4^4(10)$ hydrogen bonding ring motif which both pre-organises an $N_2O_2$ donor-set towards binding of planar transition metal ions, and stabilises the

complexes after they have formed. The size of the cavity at the centre of the pseudomacrocycle is known to influence the binding-selectivity of metal ions, and the aim of this study was to investigate the extent to which the size of this cavity (and presumably metal-ion selectivity) can be varied with pressure.

The crystal structures at ambient pressure show that the size of the cavity varies according to the ligand occupying the 3-position of the salicylaldoxime ring. The smallest cavity was observed for the OMe derivative, and H-bonding analysis combined with PIXEL calculations were used to show that interligand H-bonding involving the OMe group (see Figure 7) supports the H-bonds of the $R_4^4(10)$ ring, so reducing the cavity size. The largest cavity was observed for the $^t$Bu derivative, and could be ascribed to steric effects.

Crystal structures for each derivative were determined between 0 and 5-6 GPa. In each case the pseudo-macrocyclic cavity decreases smoothly with the application of pressure. The combination of varying the nature of the 3-substituent and of changing the pressure can change the $N_2O_2$ cavity radius between 1.87 and 2.04 Å. This range spans the covalent radii of many of the 1$^{st}$ transition series metal dications and may allow the selectivity of metal extraction to be tuned using a combination of chemical derivatisation and high pressure.

**References**


[1] I. D. H. Oswald, D. R. Allan, W. D. S. Motherwell and S. Parsons, *Acta Crystallographica, Section B*, 2005, **61**, 69-79.

[2] E. V. Boldyreva, *Journal of Molecular Structure*, 2004, **700**, 151-155.

[3] S. A. Moggach, D. R. Allan, S. Parsons and L. Sawyer, *Acta Crystallographica, Section B*, 2006, **62**, 310-320.

[4] C. H. Gorbitz, *Acta Crystallographica, Section B*, 2002, **58**, 849-854.

[5] R. W. H. Small, *Acta Crystallographica, Section B*, 2003, **59**, 141-148

[6] G. W. Gokel, *Crown Ethers and Cryptands*, The Royal Society of Chemistry, Cambridge, UK, 1991.

[7] A. G. Smith, P. A. Tasker and D. J. White, *Coordination Chemistry Reviews*, 2002, **241**, 61-85.

[8] G. A. Kordosky, *Proceedings of the International Solvent Extraction Conference*, South African Institute of Mining and Metallurgy, Cape Town, 2002, 853-862.

[9] P. A. Wood, R. S. Forgan, D. Henderson, S. Parsons, E. Pidcock, P. A. Tasker and J. E. Warren, *Acta Crystallographica, Section B*, 2006, **62**, 1099-1111.

[10] J. Szymanowski, *Hydroxyoximes and Copper Hydrometallurgy*, CRC Press, London, UK, 1993.

[11] D. Stepniak-Biniakiewicz, *Polish Journal of Chemistry*, 1980, **54**, 1567-1571.

[12] N. U. Hofslokken and L. Skattebol, *Acta Chemica Scandinavica*, 1999, **53**, 258-262.

[13] R. S. Forgan, P. A. Wood, J. Campbell, D. K. Henderson, F. E. McAllister, S. Parsons, E. Pidcock, R. Swart and P. A. Tasker, *Chemical Communications*, 2007, Advance article.

[14] L. Merrill and W. A. Bassett, *Review of Scientific Instruments*, 1974, **45**, 290-294.

[15] G. J. Piermarini, S. Block, J. D. Barnett and R. A. Forman, *Journal of Applied Physics*, 1975, **46**, 2774-2780.

[16] A. Dawson, D. R. Allan, S. Parsons and M. Ruf, *Journal of Applied Crystallography*, 2004, **37**, 410-416.

[17] S. A. Moggach, D. R. Allan, S. Parsons, L. Sawyer and J. E. Warren, *Journal of Synchrotron Radiation*, 2005, **12**, 598-607.

[18] Bruker-Nonius, *SAINT version 7*, *Program for integration of area detector data*. Bruker-AXS, Madison, Wisconsin, USA, 2006.

[19] S. Parsons, *SHADE*, *Program for empirical absorption corrections to high pressure data*. The University of Edinburgh, Edinburgh, United Kingdom, 2004.

[20] G. M. Sheldrick, *SADABS Version 2004-1*, *Program for absorption corrections to area detector data*. Bruker-AXS, Madison, Wisconsin, USA, 2004.

[21] P. W. Betteridge, J. R. Carruthers, R. I. Cooper, K. Prout and D. J. Watkin, *Journal of Applied Crystallography*, 2003, **36**, 1487.

[22] I. J. Bruno, J. C. Cole, P. R. Edgington, M. Kessler, C. F. Macrae, P. McCabe, J. Pearson and R. Taylor, *Acta Crystallographica, Section B*, 2002, **58**, 389-397.

[23] Crystal Impact, *DIAMOND version 3.0*, *Visual crystal structure information system*. Crystal Impact GbR, Postfach 1251, 53002, Bonn, Germany, 2004.

[24] A. L. Spek, *Journal of Applied Crystallography*, 2003, **36**, 7-13.

[25] L. J. Farrugia, *Journal of Applied Crystallography*, 1999, **32**, 837-838.

[26] F. H. Allen, *Acta Crystallographica, Section B*, 2002, **58**, 380-388.

[27] F. H. Allen and W. D. S. Motherwell, *Acta Crystallographica, Section B*, 2002, **58**, 407-422.

[28] R. J. Angel, *Reviews in Mineralogy and Geochemistry*, 2000, **41**, 35-59.

[29] M. J. Frisch, G. W. Trucks, H. B. Schlegel, G. E. Scuseria, M. A. Robb, J. R. Cheeseman, V. G. Zakrzewski, J. A. J. Montgomery, R. E. Stratmann, J. C. Burant, S. Dapprich, J. M. Millam, A. D. Daniels, K. N. Kudin, M. C. Strain, O. Farkas, J. Tomasi, V. Barone, M. Cossi, R. Cammi, B. Mennucci, C. Pomelli, C. Adamo, S. Clifford, J. Ochterski, G. A. Petersson, P. Y. Ayala, Q. Cui, K. Morokuma, D. K. Malick, A. D. Rabuck, K. Raghavachari, J. B. Foresman, J. Cioslowski, J. V. Ortiz, B. B. Stefanov, G. Liu, A. Liashenko, P. Piskorz, I. Komaromi, R. Gomperts, R. L. Martin, D. J. Fox, T. Keith, M. A. Al-Laham, C. Y. Peng, A. Nanayakkara, C. Gonzalez, M. Challacombe, P. M. W. Gill, B. G. Johnson, W. Chen, M. W. Wong, J. L. Andres, M. Head-Gordon, E. S. Replogle and J. A. Pople, *Gaussian 98 revision A.7*. Gaussian, Inc., Pittsburgh, PA, USA, 1998.

[30] A. Gavezzotti, *OPiX*, *A computer program package for the calculation of intermolecular interactions and crystal energies*. University of Milano, Milan, Italy, 2003.

[31] A. Gavezzotti, *Zeitschrift fuer Kristallographie*, 2005, **220**, 499-510.

[32] J. D. Dunitz and A. Gavezzotti, *Angewandte Chemie, International Edition*, 2005, **44**, 1766-1787.

[33] T. Xu, L.-z. Li and H.-w. Ji, *Hecheng Huaxue*, 2004, **12**, 22-24.

[34] J. Bernstein, R. E. Davis, L. Shimoni and N.-L. Chang, *Angewandte Chemie, International Edition*, 1995, **34**, 1555-1573.

[35] F. Birch, *Physical Review*, 1947, **71**, 809-824.

[36] R. J. Angel, R. T. Downs and L. W. Finger, *Reviews in Mineralogy and Geochemistry*, 2000, **41**, 559-596.

[37] C. Slebodnick, J. Zhao, R. Angel, B. E. Hanson, Y. Song, Z. Liu and R. J. Hemley, *Inorganic Chemistry*, 2004, **43**, 5245-5252.

[38] A. Gavezzotti, *Structural Chemistry*, 2005, **16**, 177-185.

[39] A. Gavezzotti, 2007, personal communication.